

# Exploring potential of OpenAI o3 as a signal-agnostic model for Signal/Background separation in $t \rightarrow uZ$ FCNC Searches at Future Hadron Colliders

---

Saqlain, A.<sup>1</sup> and Kartal, S.

*Istanbul University,  
Istanbul, Türkiye*

*E-mail:* [a.saqlain@ogr.iu.edu.tr](mailto:a.saqlain@ogr.iu.edu.tr), [sehban@istanbul.edu.tr](mailto:sehban@istanbul.edu.tr)

**ABSTRACT:** We present a case study exploring the potential of OpenAI's o3 model as a signal-agnostic tool for predicting optimized selection cuts in high-energy physics analyses. Specifically, we investigate the effectiveness of the model in separating signal from relevant Standard Model backgrounds in the context of Flavour-Changing Neutral Current (FCNC) top-quark couplings, focusing on the rare decay process  $t \rightarrow uZ$ . The study is performed at three collider setups: the approved High-Luminosity LHC (HL-LHC), the proposed High-Energy LHC (HE-LHC), and the Future Circular Collider in hadron-hadron mode (FCC-hh). We train the o3 model on detector level data for signal and background processes to predict selection cuts that enhance Signal-to-Background (S/B) discrimination. A comparative analysis is then carried out between the efficiencies resulting from o3-predicted cuts and those derived from traditional manually designed strategies used by a control group. Our results demonstrate that the o3 model performs on par with traditional methods in terms of S/B separation, with a slight improvement in the case of FCC-hh, suggesting its promise as a fast and generalizable tool for new physics searches.

---

<sup>1</sup>Corresponding author.

---

## Contents

<b>1</b>	<b>Introduction</b>	<b>1</b>
<b>2</b>	<b>Theoretical Background</b>	<b>2</b>
<b>3</b>	<b>Event generation</b>	<b>3</b>
<b>4</b>	<b>Analysis</b>	<b>5</b>
<b>5</b>	<b>Comparative Analysis</b>	<b>8</b>
<b>6</b>	<b>Conclusions</b>	<b>10</b>

---

## 1 Introduction

Although the Standard Model (SM) has been remarkably successful in describing a wide range of particle physics phenomena, it still has certain limitations. [1], physicists often explore the limits of particle physics by proposing and testing various Beyond the Standard Model (BSM) processes. One of these BSM processes is the top-quark Flavour-Changing Neutral Current (FCNC) interaction  $t \rightarrow uZ$  which will be the focus of this research. In the SM, this decay is forbidden at tree level and highly suppressed at the loop level due to the Glashow–Iliopoulos–Maiani (GIM) mechanism [2–4], with its branching ratio predicted to be of order  $10^{-14}$  [5], placing it well below the current LHC reach. However, many BSM models predict  $\text{BR}(t \rightarrow qZ)$  to lie in the range  $10^{-4}$ – $10^{-7}$ . Examples include the 2-Higgs–Doublet Model (2HDM), the quark-singlet model, the Minimal Supersymmetric Standard Model (MSSM) and its extensions, extended mirror-fermion models, and warped extra-dimensions models [6–11]. Therefore, the  $tZ$  FCNC process serves as a sensitive probe of BSM physics [12, 13]. It is to be noted that, to date, no evidence of top-quark FCNC interactions has been observed, but one must not disregard its discovery potential at the proposed Future Colliders like the High-Luminosity LHC (HL-LHC) with an Integrated Luminosity ( $L_{int}$ ) of  $3 \text{ ab}^{-1}$  and a Centre-of-Mass energy ( $\sqrt{s}$ ) of 14 TeV [14], High-Energy LHC (HE-LHC) with  $L_{int} = 15 \text{ ab}^{-1}$  and  $\sqrt{s} = 27 \text{ TeV}$  [15] and lastly the Future Circular Collider in hadron–hadron mode (FCC-hh), which will operate at  $\sqrt{s} = 100 \text{ TeV}$  with  $L_{int} = 30 \text{ ab}^{-1}$  [16].

As with any rare signal, the first step in a detailed study is to isolate it by separating the BSM signal from all relevant SM backgrounds. Since the 1990s, Machine Learning (ML) techniques have significantly contributed to particle-physics analyses, especially for Signal/Background (S/B) separation. The most common ML practice nowadays utilizes the Toolkit for MultiVariate Analysis (TMVA) package [17] within ROOT [18] to

train Boosted Decision Trees (BDTs) via AdaBoost. Other frequently used algorithms include  $k$ -nearest neighbours, random forests, and support-vector machines from the SCIKIT-LEARN library [19], and neural networks implemented via PyTorch [20], TensorFlow [21], Theano [22], Microsoft Cognitive Toolkit (CNTK) [23], and Keras [24]. For a more comprehensive review of ML applications in particle physics, see Ref. [25].

Since ML models are generally signal-specific, there is a rising need to modify them so that they become signal-agnostic [26] and can be applied across multiple new-physics scenarios. In this study, we explore that trend by testing the effectiveness of OpenAI’s latest and most advanced o3 model [27] as a candidate for S/B separation. We use Ref. [28] as a benchmark, adopting the  $ug \rightarrow tZ$  process as our signal (case B in [28]) and treating  $t\bar{t}$ ,  $t\bar{t}W$ ,  $t\bar{t}Z$ , and  $WZ$  as background events. Our goal is to evaluate o3’s effectiveness and adaptability, since it is not a particle-physics-specific model but rather part of a broader Large Language Model (LLM) family. Our objective is to assess whether such a model can function as a signal-agnostic classifier, defined here as the ability to distinguish signal events from background processes based solely on detector-level signatures, without prior knowledge of the signal’s underlying physics. This study explores the potential of o3 to fulfill this role, thereby evaluating the broader applicability of LLMs in high-energy physics analyses. Recent studies have shown o3’s superiority in competitive-programming tasks [29] as well, making it an attractive prototype for an S/B separation model that is time-efficient, easily trainable on new datasets, computationally efficient, and accurate in its analyses.

This study comprises two main steps. First, we replicate the reference analysis, generating the relevant signal and background samples at HL-LHC, HE-LHC and FCC-hh energies, and discuss this in detail in Sections.2 and 3. Second, we employ the o3 model to predict optimal selection cuts, apply them to our dataset, and compare the results against our control group in terms of effectiveness. This workflow is covered in Section.4 and 5, and finally we conclude our results in Section.6 at the end.

## 2 Theoretical Background

For this study, we focused on the  $tZ$  production which utilized the  $tZq$  FCNC ( $q = u$ ) anomalous couplings. The  $tZ$ , after production, further decays into 3 leptons (including an Opposite-sign, Same-Flavor (OSSF) pair) and 1 b-tagged jet as shown in figure 1.

The SM model is expanded by using an effective field theory approach which incorporates the  $tZq$  ( $l\nu b l^+ l^-$ ) FCNC anomalous couplings [30]. The interaction between  $Z$  boson, the top quark and an up can be described by the effective Lagrangian as [30]:

$$\begin{aligned} \mathcal{L}_{\text{eff}} = \sum_{q=u,c} \left[ \frac{g}{4c_W m_Z} \kappa_{tqZ} \bar{q} \sigma^{\mu\nu} (\kappa_L P_L + \kappa_R P_R) t Z_{\mu\nu} \right. \\ \left. + \frac{g}{2c_W} \lambda_{tqZ} \bar{q} \gamma^\mu (\lambda_L P_L + \lambda_R P_R) t Z_\mu \right] + \text{h.c.} \end{aligned} \quad (2.1)$$

here, the  $c_W = \cos \theta_W$  and  $\theta_W$  represents the Weinberg angle,  $P_{L,R}$  are the left and right-handed chirality projector operators while the effective coupling of the vertices is

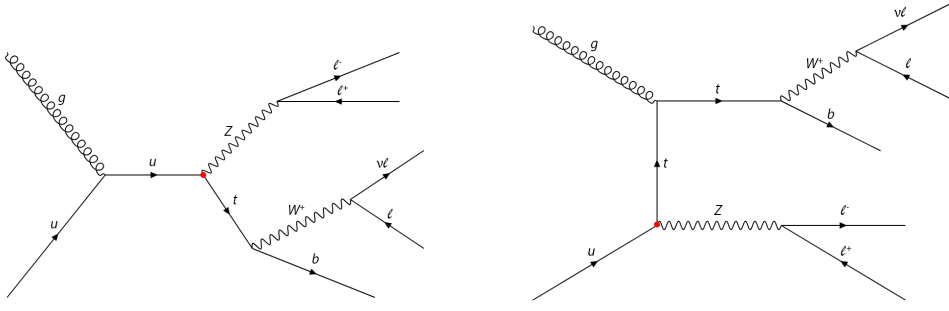


**Figure 1:** Feynman diagrams representing the  $ug \rightarrow tZ$  production and decay via the  $tZq$  FCNC anomalous couplings

represented by  $\kappa_{tqZ}$  and  $\lambda_{tqZ}$ .  $\kappa_{L,R}$  and  $\lambda_{L,R}$  represent the complex chiral parameters and are normalized as  $|\kappa_R|^2 + |\kappa_L|^2 = |\lambda_R|^2 + |\lambda_L|^2 = 1$ , whereas the coupling constant  $g$  and  $\theta_W$  govern the Electro-Weak (EW) interaction.

Following the same step as the reference study [28], the partial widths for the two tensor variables in the above equation, are calculated by

$$\begin{aligned}\Gamma(t \rightarrow qZ)_{\sigma^{\mu\nu}} &= \frac{\alpha}{128 s_W^2 c_W^2} |\kappa_{tqZ}|^2 \frac{m_t^3}{m_Z^2} \left[1 - \frac{m_Z^2}{m_t^2}\right]^2 \left[2 + \frac{m_Z^2}{m_t^2}\right], \\ \Gamma(t \rightarrow qZ)_{\gamma^{\mu}} &= \frac{\alpha}{32 s_W^2 c_W^2} |\lambda_{tqZ}|^2 \frac{m_t^3}{m_Z^2} \left[1 - \frac{m_Z^2}{m_t^2}\right]^2 \left[1 + 2 \frac{m_Z^2}{m_t^2}\right].\end{aligned}\tag{2.2}$$

Agreeing with the SM assumption of dominant top decay to be  $t \rightarrow bW^+$  [31]

$$\Gamma(t \rightarrow bW^+) = \frac{\alpha}{16 s_W^2} |V_{tb}|^2 \frac{m_t^3}{m_W^2} \left[1 - 3 \frac{m_W^4}{m_t^4} + 2 \frac{m_W^6}{m_t^6}\right],\tag{2.3}$$

while neglecting the light quark masses, the BR can be calculated as directly dependent on the effective coupling constants [3]:

$$\begin{aligned}\text{BR}(t \rightarrow qZ)_{\sigma^{\mu\nu}} &= 0.172 |\kappa_{tqZ}|^2, \\ \text{BR}(t \rightarrow qZ)_{\gamma^{\mu}} &= 0.471 |\lambda_{tqZ}|^2.\end{aligned}\tag{2.4}$$

In the above calculation, the Next-to-Leading-Order (NLO) QCD correction of top quark decay are also included in a model-independent FCNC framework and the  $k$ -factor is taken as 1.02 [32, 33]. The relationship between the cross section  $\sigma$  and  $\kappa_{tqZ}$ ,  $\lambda_{tqZ}$  is highlighted in figure 2

### 3 Event generation

The signal utilized for this study is given as:

$$pp \rightarrow tZ, (t \rightarrow bW^+ \rightarrow bl^+v), (Z \rightarrow l^+l^-),\tag{3.1}$$

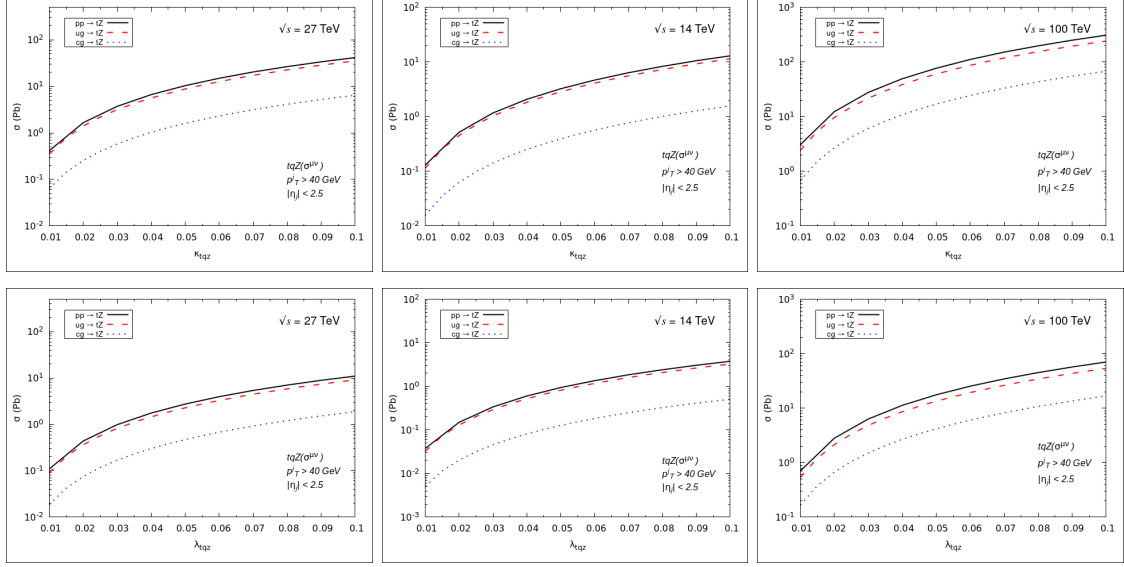


**Figure 2:** The variation of the cross section  $\sigma$  (in pb) with respect to the FCNC couplings  $\kappa_{tqZ}$  (top row) and  $\lambda_{tqZ}$  (bottom row) is illustrated for three collider scenarios: HL-LHC (left), HE-LHC (center), and FCC-hh (right). All results are obtained via basic cuts of  $p_T^j > 40$  GeV and  $|\eta_j| < 2.5$ .

here,  $l = \mu, e$ . This also includes the charge-conjugate channel ( $pp \rightarrow \bar{t}Z$ ) as well and the signal, overall, is characterized by the decay of 3 leptons, a  $b$ -jet and Missing Transverse Energy (MET) due to the presence of a neutrino from the decay of  $W^\pm$ . The main backgrounds we are going to be considering are  $t\bar{t}$ ,  $t\bar{t}W$ ,  $t\bar{t}Z$ , and  $WZ$ , all decayed leptonically into electrons and muons.

For the simulation of the signal, we implement the FeynRules package [34] to generate the Universal FeynRules Output (UFO) files [35]. Madgraph5\_aMC@nlo [36] was employed to generate the signal using the NNPDF23L01 Parton Distribution Functions (PDFs) [37] while taking the renormalization and factorization scales to be  $\mu_R = \mu_F = \mu_0/2 = (m_t + m_Z)/2$ . You can find the value of other parameters below:

$$\begin{aligned}
 m_t &= 173.1 \text{ GeV}, & m_Z &= 91.1876 \text{ GeV}, \\
 m_W &= 80.379 \text{ GeV}, & \alpha_s(m_Z) &= 0.1181, \\
 G_F &= 1.16637 \times 10^{-5} \text{ GeV}^{-2}.
 \end{aligned} \tag{3.2}$$

Both the signal and background processes, after being generated at LO from Madgraph5\_aMC@nlo, are forwarded to Pythia 8.3 [38] framework for hadronization. FASTJET 3.2 [39] was utilized for jet clustering with the anti- $k_t$  algorithm with a cone radius of  $R=0.4$  [40]. Afterwards the events were driven through Delphes 3.5.0 [41] to implement detector effects using the default HL-LHC, HE-LHC and FCC-hh cards. At the end, MadAnalysis5 [42] is used to do the event analysis.

We re-normalize the LO cross sections for the signal to the corresponding higher order QCD results presented in Refs. [43–45]. Meanwhile, the SM background cross sections are

re-normalized to the NLO or Next-NLO (NNLO) order cross sections using Refs. [46–53].

## 4 Analysis

All the event root files (signal + background), obtained from Delphes, are converted to Les Houches Collider Output (.lhco) format using root2lhco [54] framework. The events are then further split into 2 data sets, training data set and analysis data set. Training data set consists of 10k events for each signal and background processes, totaling up to 50k events while the analysis data set consist of events normalized to the luminosity of each collider respectively.

Some Basic cuts are applied on both data sets in order to identify objects, defined in the control group article [28] as:

$$\begin{aligned} p_T^\ell &> 25 \text{ GeV}, \quad p_T^{j/b} > 30 \text{ GeV}, \quad |\eta_i| < 2.5, \\ \Delta R_{ij} &> 0.4, \quad (i, j = \ell, b, j), \end{aligned} \quad (4.1)$$

Below are the cuts defined in the control paper [28]:

- (Cut 1) There are three leptons, among which at least two have positive charge and  $P_T > 30 \text{ GeV}$ , and there is exactly one  $b$ -tagged jet with  $P_T > 40 \text{ GeV}$ ; the event is rejected if the  $P_T$  of the sub-leading jet is greater than  $25 \text{ GeV}$ .
- (Cut 2) The distance between the OSSF lepton pair should lie within  $\Delta R(l_1, l_2) \in [0.2, 1.3]$  while the corresponding invariant mass is required to be  $|M[l_1, l_2] - m_Z| < 15 \text{ GeV}$ .
- (Cut 3) The transverse masses of the reconstructed  $W^\pm$  boson and top quark masses are required to satisfy  $50 \text{ GeV} < M_T^{l3} < 100 \text{ GeV}$  and  $100 \text{ GeV} < M_T^{l3} < 200 \text{ GeV}$ , respectively.
- (Cut 4) The rapidity of the OSSF lepton pair is required to be  $|y_{\ell_1 \ell_2}| > 1.0$ .

The effects of the cut selection from the control group are given in the Tables 1,2 and 3 respectively.

**Table 1:** Cut flow for the  $ug \rightarrow tZ$  signal and background cross sections (in  $\times 10^{-2} \text{ fb}$ ) at HL-LHC with  $\kappa_{tqZ} = 0.1$  and  $\lambda_{tqZ} = 0.1$ , based on the cuts proposed by the control group.

Cuts	Signal		Backgrounds		
	$ug \rightarrow tZ$	$WZ$	$t\bar{t}$	$t\bar{t}Z$	$t\bar{t}W$
Basic	4221	474	$2.2 \times 10^6$	602	233
Cut 1	272.57	23.46	1196.97	2.83	7.12
Cut 2	140.35	4.51	11.22	0.57	0.071
Cut 3	84.895	1.13	2.83	0.11	0.019
Cut 4	48.55	0.24	1.21	0.034	0.009

**Table 2:** Cut flow for the  $ug \rightarrow tZ$  signal and background cross sections (in fb) at HE-LHC with  $\kappa_{tqZ} = 0.1$  and  $\lambda_{tqZ} = 0.1$ , based on the cuts proposed by the control group.

Cuts	Signal	Backgrounds			
	$ug \rightarrow tZ$	$WZ$	$t\bar{t}$	$t\bar{t}Z$	$t\bar{t}W$
Basic	153	14.2	64628	31.6	7.7
Cut 1	7.47	0.476	0.823	0.06	0.089
Cut 2	4.1	0.07	0.017	0.014	0.0008
Cut 3	2.3	0.02	0.003	0.002	0.0002
Cut 4	1.5	0.013	0	0.0007	$6.7 \times 10^{-5}$

**Table 3:** Cut flow for the  $ug \rightarrow tZ$  signal and background cross sections (in fb) at FCC-hh with  $\kappa_{tqZ} = 0.1$  and  $\lambda_{tqZ} = 0.1$ , based on the cuts proposed by the control group.

Cuts	Signal	Backgrounds			
	$ug \rightarrow tZ$	$WZ$	$t\bar{t}$	$t\bar{t}Z$	$t\bar{t}W$
Basic	951	313	697297	242	43
Cut 1	24.1	3.77	4.98	0.33	13.38
Cut 2	12.57	0.49	0	0.067	0.131
Cut 3	7.52	0.24	0	0.006	0.022
Cut 4	5.157	0.17	0	0.003	0.017

Whereas for obtaining the cuts from the o3 model, we directly provided model access to the training data set by utilizing the project feature on the OpenAI’s ChatGPT interface. Afterwards, The model was provided with the following key information:

- The label of every `.lhco` file and what processes are in it.
- Information about the `.lhco` format, syntax and representation of particles inside it.
- Full decay chain of each of the processes.
- Information about the value of other applicable parameters

Then it was prompted to define cuts on each parameter one by one, in separate prompts, with the goal of maximizing signal events while minimizing background ones. The reason for defining the cuts one by one instead of all at once is because it was observed that the model was overwhelmed when asked to define all the cuts at once on all parameters and was not able to go through the data efficiently. This approach mimics how a human analyst might iteratively explore variables to find optimal thresholds. All the prompts and the o3 analysis methodology can be found in this reference [55]. The parameters below represent the parameters on which the cuts were applied in the control paper. These include:

1. Number (N), Charge (Q) and Transverse Momentum ( $p_T$ ) of leptons and b-jets
2. Angular distance ( $\Delta R$ ) of the OSSF lepton pair and the invariant mass of  $Z$ .

3. Transverse Mass ( $M_T$ ) of  $W$  Boson and  $t$  quark.
4. Rapidity of the OSSF lepton pair.

The o3 model defined the below given cuts for the effective separation of the signal from background events:

- (Cut 1) Exactly 3 leptons with two having a positive charge, the requirement for  $P_T$  of leading lepton is  $P_T^{l_1} > 200$  GeV, of sub-leading lepton is  $P_T^{l_2} > 60$  GeV and for the  $b$  quarks is  $P_T^b > 120$  GeV.
- (Cut 2) The distance of the OSSF lepton pair should be  $\Delta R(l_1, l_2) \in [0.2, 1.0]$  and the invariant mass of  $Z$  boson is defined as  $88 \text{ GeV} < |M[l_1, l_2]| < 95 \text{ GeV}$ .
- (Cut 3)  $M_T$  of top quark is required to be  $M_T^{bl_3} < 180$  GeV and that of  $W^\pm$  boson is  $30 \text{ GeV} < M_T^{l_3} < 100$  GeV.
- (Cut 4) The Rapidity of the OSSF pair is required to be  $|y_{\ell_1 \ell_2}| > 2.0$ .

The resulting cross section cuts effect for the o3 model are given in Tables 4, 5 and 6.

**Table 4:** Cut flow for the  $ug \rightarrow tZ$  signal and background cross sections (in  $\times 10^{-2}$  fb) at HL-LHC with  $\kappa_{tqZ} = 0.1$  and  $\lambda_{tqZ} = 0.1$ , based on the cuts proposed by o3 model.

Cuts	Signal	Backgrounds			
	$ug \rightarrow tZ$	$WZ$	$t\bar{t}$	$t\bar{t}Z$	$t\bar{t}W$
Basic	4221	474	$2.2 \times 10^6$	602	233
Cut 1	172.91	1.88	207.35	4.16	1.18
Cut 2	83.38	0.44	0.27	1.18	0.0009
Cut 3	51.96	0	0	0.201	$5.5 \times 10^{-5}$
Cut 4	45.62	0	0	0.199	$5.5 \times 10^{-5}$

**Table 5:** Cut flow for the  $ug \rightarrow tZ$  signal and background cross sections (in fb) at HE-LHC with  $\kappa_{tqZ} = 0.1$  and  $\lambda_{tqZ} = 0.1$ , based on the cuts proposed by o3 model.

Cuts	Signal	Backgrounds			
	$ug \rightarrow tZ$	$WZ$	$t\bar{t}$	$t\bar{t}Z$	$t\bar{t}W$
Basic	153	14.2	64628	31.6	7.7
Cut 1	7.41	0.105	0.05	0.36	0.12
Cut 2	3.4	0.04	0	0.1	0.0002
Cut 3	2.02	0.001	0	0.014	$1.68 \times 10^{-5}$
Cut 4	1.53	0.001	0	0.013	$1.68 \times 10^{-5}$

The o3 model was able to perform high-level reasoning in understanding the event topology, and proposing relevant selection cuts. During the iterative prompting, it adapted its cut suggestions based on histogram feedback and performance summaries, rechecking the variables and efficiencies of signal and backgrounds based on previous iteration of cuts.

**Table 6:** Cut flow for the  $ug \rightarrow tZ$  signal and background cross sections (in fb) at FCC-hh with  $\kappa_{tqZ} = 0.1$  and  $\lambda_{tqZ} = 0.1$ , based on the cuts proposed by o3 model.

Cuts	Signal	Backgrounds			
	$ug \rightarrow tZ$	$WZ$	$t\bar{t}$	$t\bar{t}Z$	$t\bar{t}W$
Basic	951	313	697297	242	43
Cut 1	62.81	3.603	124.18	1.65	11.32
Cut 2	27.53	0.898	0	0.43	0.2
Cut 3	16.3	0	0	0.07	0.006
Cut 4	9.06	0	0	0.058	0

It was able to parse through the files efficiently, binning the entries and tabulating them after each cut to adjust its strategy, even providing multiple cuts based on the strength of the cut on the background events.

## 5 Comparative Analysis

In this section, we will define some statistical metrics which provide us a better understanding as to the effectiveness of the Analysis done by the o3 and the control group.

A basic S/B efficiency comparison, utilizing

$$S/B \text{ Efficiency} = \frac{S}{\sqrt{S+B}} \quad (5.1)$$

for each cut is given in Table 7, 8 and 9.

**Table 7:** Comparative Analysis of the S/B efficiencies for each Analysis at HL-LHC energies.

Cuts	Efficiency (Control Group)	Efficiency (o3 Model)
Basic	2.34	2.34
Cut 1	4.79	5.46
Cut 2	13.36	6.79
Cut 3	15.78	9.63
Cut 4	14.01	8.59

It was observed that the cuts proposed by the o3 model allowed the  $t\bar{t}Z$  background to slip through which is the main cause of the slightly worse S/B efficiency for the o3 model.

An approximate Receiver-Operating Characteristic (ROC) curve is also given in figure 3 for all the three collider energies by taking True Positive Rate (TPR) as Signal Efficiency ( $\epsilon_s$ ) and Background Efficiency ( $\epsilon_b$ ) as False Positive Rate (FPR). where:

$$\epsilon_s = \frac{S_{after \text{ cut}}}{S_{initial}} \quad , \quad \epsilon_b = \frac{B_{after \text{ cut}}}{B_{initial}} \quad (5.2)$$

**Table 8:** Comparative Analysis of the S/B efficiencies for each Analysis at HE-LHC energies.

Cuts	Efficiency (Control Group)	Efficiency (o3 Model)
Basic	9.84	9.84
Cut 1	8.04	5.82
Cut 2	20.87	8.2
Cut 3	23.27	12.17
Cut 4	21.91	9.5

**Table 9:** Comparative Analysis of the S/B efficiencies for each Analysis at FCC-hh energies.

Cuts	Efficiency (Control Group)	Efficiency (o3 Model)
Basic	2.73	2.73
Cut 1	8.64	21.07
Cut 2	14.39	21.87
Cut 3	14.38	23.55
Cut 4	12.54	16.88

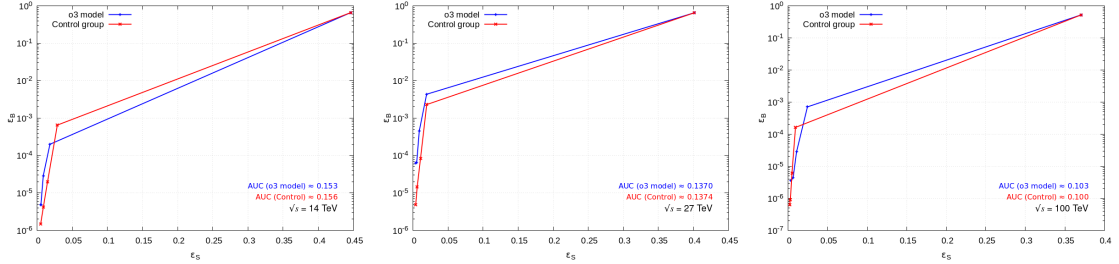


**Figure 3:** ROC curve comparison between cuts defined by both Analyses at different collider energies

F1 Score for both analyses is also calculated and tabulated in the table 10 in order to measure the performance accuracy of both set of analyses, by taking  $Recall = \epsilon_s$ . Both precision (utilized for calculation of F1 score) and F1 score are defined by:

$$Precision = \frac{n_S}{n_S + n_B} \quad , \quad F1 = 2 \cdot \frac{Precision \cdot Recall}{Precision + Recall} \quad (5.3)$$

here  $n_S$  and  $n_B$  is the total number of signal and backgrounds that survived all the cuts respectively.

**Table 10:** F1 scores for both Analysis at different collider energies

Collider	F1 (Control Group)	F1 (o3 model)
HL-LHC	0.010124	0.009346
HE-LHC	0.00779	0.007754
FCC-hh	0.00401	0.007019

## 6 Conclusions

In this study, we analyzed the efficiency of cuts proposed by the o3 model with respect to those proposed by the control group on the FCNC  $t \rightarrow uZ$  anomalous couplings for the signal at HL-LHC, HE-LHC, and FCC-hh energies. We trained the o3 model on a training set of 50k events in total, in `.lhco` format, and then used it to predict selection cuts. We performed a comparative analysis of the efficiency of the signal and relevant SM background cuts from the control group and those predicted by the o3 model. In just under 20 minutes of analysis, the o3 model was able to provide cuts that were comparable to the control group cut selections if not superior in the case of FCC-hh. This does not diminish the significant fact that o3, despite not being a model specifically designed for particle physics, was able to perform accurate signal separation and may serve as a precursor to a new generation of signal-agnostic models for future analyses.

## Acknowledgments

The numerical calculations reported in this paper were fully/partially performed at TUBITAK ULAKBIM, High Performance and Grid Computing Center (TRUBA resources).

## References

- [1] S.F. Novaes, *Standard model: An introduction*, 2000.
- [2] S.L. Glashow, J. Iliopoulos and L. Maiani, *Weak Interactions with Lepton-Hadron Symmetry*, *Phys. Rev. D* **2** (1970) 1285.
- [3] J. Aguilar-Saavedra, *35.2695 a. vol. 35*, 2004.
- [4] J.A. Aguilar-Saavedra, *A minimal set of top-higgs anomalous couplings*, *Nuclear physics B* **821** (2009) 215.
- [5] K. Agashe, R. Erbacher, C.E. Gerber, K. Melnikov, R. Schwienhorst, A. Mitov et al., *Snowmass 2013 top quark working group report*, 2013.
- [6] D. Atwood, L. Reina and A. Soni, *Phenomenology of two higgs doublet models with flavor-changing neutral currents*, *Phys. Rev. D* **55** (1997) 3156.
- [7] V. Barger, M.S. Berger and R.J.N. Phillips, *Quark singlets: Implications and constraints*, *Physical Review D* **52** (1995) 1663–1683.

- [8] J.J. Cao, G. Eilam, M. Frank, K. Hikasa, G.L. Liu, I. Turan et al., *Supersymmetry-induced flavor-changing neutral-current top-quark processes at the cern large hadron collider*, *Phys. Rev. D* **75** (2007) 075021.
- [9] J.M. Yang, B.-L. Young and X. Zhang, *Flavor-changing top quark decays in r-parity-violating supersymmetric models*, *Phys. Rev. D* **58** (1998) 055001.
- [10] P. Hung, Y.-X. Lin, C.S. Nugroho and T.-C. Yuan, *Top quark rare decays via loop-induced  $fcnc$  interactions in extended mirror fermion model*, *Nuclear Physics B* **927** (2018) 166.
- [11] K. Agashe, G. Perez and A. Soni, *Collider signals of top quark flavor violation from a warped extra dimension*, *Physical Review D—Particles, Fields, Gravitation, and Cosmology* **75** (2007) 015002.
- [12] T.M. Tait and C.-P. Yuan, *Single top quark production as a window to physics beyond the standard model*, *Physical Review D* **63** (2000) 014018.
- [13] J. Aguilar-Saavedra and G.C. Branco, *Probing top flavour-changing neutral scalar couplings at the cern lhc*, *Physics Letters B* **495** (2000) 347.
- [14] O. Aberle, I. Béjar Alonso, O. Brüning, P. Fessia, L. Rossi, L. Tavian et al., *High-Luminosity Large Hadron Collider (HL-LHC): Technical design report*, CERN Yellow Reports: Monographs, CERN, Geneva (2020), [10.23731/CYRM-2020-0010](https://arxiv.org/abs/10.23731/CYRM-2020-0010).
- [15] M. Benedikt and F. Zimmermann, *Proton colliders at the energy frontier*, *Nuclear Instruments and Methods in Physics Research Section A: Accelerators, Spectrometers, Detectors and Associated Equipment* **907** (2018) 200.
- [16] N. Arkani-Hamed, T. Han, M. Mangano and L.-T. Wang, *Physics opportunities of a 100 tev proton-proton collider*, *Physics Reports* **652** (2016) 1.
- [17] A. Hoecker, P. Speckmayer, J. Stelzer, J. Therhaag, E. von Toerne, H. Voss et al., *Tmva-toolkit for multivariate data analysis*, *arXiv preprint physics/0703039* (2007) .
- [18] R. Brun, F. Rademakers, P. Canal, A. Naumann, O. Couet, L. Moneta et al., *root-project/root: v6.18/02 (v6-18-02)*, 2019. 10.5281/zenodo.3895860.
- [19] F. Pedregosa, G. Varoquaux, A. Gramfort, V. Michel, B. Thirion, O. Grisel et al., *Scikit-learn: Machine learning in python, the Journal of machine Learning research* **12** (2011) 2825.
- [20] A. Paszke, *Pytorch: An imperative style, high-performance deep learning library*, *arXiv preprint arXiv:1912.01703* (2019) .
- [21] M. Abadi, A. Agarwal, P. Barham, E. Brevdo, Z. Chen, C. Citro et al., *TensorFlow: Large-scale machine learning on heterogeneous systems*, 2015.
- [22] R. Al-Rfou, G. Alain, A. Almahairi, C. Angermueller, D. Bahdanau, N. Ballas et al., *Theano: A python framework for fast computation of mathematical expressions. arxiv e-prints, arxiv-1605*, 2016.
- [23] F. Seide and A. Agarwal, *Cntk: Microsoft’s open-source deep-learning toolkit*, in *Proceedings of the 22nd ACM SIGKDD international conference on knowledge discovery and data mining*, pp. 2135–2135, 2016.
- [24] F. Chollet et al., “Keras.” <https://keras.io>, 2015.
- [25] M. Feickert and B. Nachman, *A living review of machine learning for particle physics*, 2021.

- [26] G. Grosso and M. Letizia, *Multiple testing for signal-agnostic searches of new physics with machine learning*, 2024.
- [27] OpenAI, *Introducing OpenAI o3 and o4-mini*, 2025.
- [28] Y.-B. Liu and S. Moretti, *Probing  $tqz$  anomalous couplings in the trilepton signal at the  $hl\text{-}lhc$ ,  $he\text{-}lhc$ , and  $fcc\text{-}hh$  \**, *Chinese Physics C* **45** (2021) 043110.
- [29] OpenAI, :, A. El-Kishky, A. Wei, A. Saraiva, B. Minaiev et al., *Competitive programming with large reasoning models*, 2025.
- [30] J.A. Aguilar-Saavedra, *A minimal set of top anomalous couplings*, *Nuclear Physics B* **812** (2009) 181.
- [31] C.S. Li, R.J. Oakes and T.C. Yuan, *Qcd corrections to  $t \rightarrow w^{++} b$* , *Physical Review D* **43** (1991) 3759.
- [32] J.J. Zhang, C.S. Li, J. Gao, H. Zhang, Z. Li, C.-P. Yuan et al., *Next-to-leading-order qcd corrections to the top-quark decay via model-independent flavor-changing neutral-current couplings*, *Physical review letters* **102** (2009) 072001.
- [33] J. Drobnak, S. Fajfer and J.F. Kamenik, *Flavor changing neutral coupling mediated radiative top quark decays? format?; at next-to-leading order in qcd*, *Physical review letters* **104** (2010) 252001.
- [34] A. Alloul, N.D. Christensen, C. Degrande, C. Duhr and B. Fuks, *Feynrules 2.0—a complete toolbox for tree-level phenomenology*, *Computer Physics Communications* **185** (2014) 2250.
- [35] C. Degrande, C. Duhr, B. Fuks, D. Grellscheid, O. Mattelaer and T. Reiter, *Ufo—the universal feynrules output*, *Computer Physics Communications* **183** (2012) 1201.
- [36] J. Alwall, R. Frederix, S. Frixione, V. Hirschi, F. Maltoni, O. Mattelaer et al., *The automated computation of tree-level and next-to-leading order differential cross sections, and their matching to parton shower simulations*, *Journal of High Energy Physics* **2014** (2014) 1.
- [37] R.D. Ball, S. Carrazza, L. Del Debbio, S. Forte, Z. Kassabov, J. Rojo et al., *Nnpdf, Parton distributions from high-precision collider data,” Eur. Phys. J. C* **77** (2014) .
- [38] C. Bierlich, S. Chakraborty, N. Desai, L. Gellersen, I. Helenius, P. Ilten et al., *A comprehensive guide to the physics and usage of pythia 8.3*, *SciPost Physics Codebases* (2022) 008.
- [39] M. Cacciari, G.P. Salam and G. Soyez, *Fastjet user manual: (for version 3.0. 2)*, *The European Physical Journal C* **72** (2012) 1.
- [40] M. Cacciari, G.P. Salam and G. Soyez, *The anti-kt jet clustering algorithm*, *Journal of High Energy Physics* **2008** (2008) 063.
- [41] J. De Favereau, C. Delaere, P. Demin, A. Giammanco, V. Lemaitre, A. Mertens et al., *Delphes 3: a modular framework for fast simulation of a generic collider experiment*, *Journal of High Energy Physics* **2014** (2014) 1.
- [42] E. Conte, B. Fuks and G. Serret, *Madanalysis 5, a user-friendly framework for collider phenomenology*, *Computer Physics Communications* **184** (2013) 222.
- [43] B.H. Li, Y. Zhang, C.S. Li, J. Gao and H.X. Zhu, *Next-to-leading order qcd corrections to  $t z$  associated production via the flavor-changing neutral-current couplings at hadron colliders*, *Physical Review D—Particles, Fields, Gravitation, and Cosmology* **83** (2011) 114049.

- [44] C. Zhang and S. Willenbrock, *Effective-field-theory approach to top-quark production and decay*, *Physical Review D—Particles, Fields, Gravitation, and Cosmology* **83** (2011) 034006.
- [45] C. Degrande, F. Maltoni, J. Wang and C. Zhang, *Automatic computations at next-to-leading order in qcd for top-quark flavor-changing neutral processes*, *Physical Review D* **91** (2015) 034024.
- [46] A. Lazopoulos, T. McElmurry, K. Melnikov and F. Petriello, *Next-to-leading order qcd corrections to  $t\bar{t}z$  production at the lhc*, *Physics Letters B* **666** (2008) 62.
- [47] A. Kardos, Z. Trocsanyi and C. Papadopoulos, *Top quark pair production in association with a z-boson at next-to-leading-order accuracy*, *Physical Review D—Particles, Fields, Gravitation, and Cosmology* **85** (2012) 054015.
- [48] M. Czakon, P. Fiedler and A. Mitov, *Total top-quark pair-production cross section at hadron colliders through  $\mathcal{O}(\alpha_s^4)$* , *Physical Review Letters* **110** (2013) 252004.
- [49] CERN, *Cern yellow reports: Monographs, vol 3 (2017): Physics at the fcc-hh, a 100 tev pp collider*, 2017. 10.23731/CYRM-2017-003.
- [50] F. Campanario, C. Englert, S. Kallweit, M. Spannowsky and D. Zeppenfeld, *Nlo qcd corrections to  $wz+$  jet production with leptonic decays*, *Journal of High Energy Physics* **2010** (2010) 1.
- [51] J.M. Campbell and R.K. Ellis,  *$t\bar{t}w^\pm$  production and decay at nlo*, *Journal of High Energy Physics* **2012** (2012) 1.
- [52] R. Frederix, D. Pagani and M. Zaro, *Large nlo corrections in  $t\bar{t}w^\pm$  and  $t\bar{t}t\bar{t}$  hadroproduction from supposedly subleading ew contributions*, *Journal of High Energy Physics* **2018** (2018) 1.
- [53] S. Frixione, V. Hirschi, D. Pagani, H.-S. Shao and M. Zaro, *Electroweak and qcd corrections to top-pair hadroproduction in association with heavy bosons*, *Journal of High Energy Physics* **2015** (2015) 1.
- [54] A. Fowlie, *Lhco\_reader: A new code for reading and analyzing detector-level events stored in lhco format*, 2016.
- [55] A.B. Saqlain, *randomizer6542/o3-analysis: o3\_in\_out\_initial*, June, 2025. 10.5281/zenodo.15733357.